

Competition between Atmospherically Relevant Fatty Acid Monolayers at the Air/Water Interface

Laura F. Voss, Christopher M. Hadad,* and Heather C. Allen*

Department of Chemistry, The Ohio State University, 100 West 18th Avenue, Columbus, Ohio 43210

Received: April 27, 2006; In Final Form: July 2, 2006

Competition and oxidation of fatty acids spread at the air/water interface were investigated using surface-specific, broad-bandwidth, sum frequency generation spectroscopy. At the air/water interface, a monolayer of oleic acid replaced a monolayer of deuterated palmitic acid at equilibrium spreading pressure. Subsequent oxidation of the oleic acid monolayer with ozone resulted in products more water soluble than the palmitic acid; therefore, the palmitic acid monolayer reformed at the surface. Results indicate that the surfactants on the surface of fat-coated tropospheric aerosols will only possess oxidized acyl chains after all less soluble species in the aqueous subphase have been removed through the processes of replacement at the surface and atmospheric oxidation.

Introduction

The possibility that seawater aerosols injected into the atmosphere through mechanical processes may possess a hydrophobic organic monolayer was first proposed by Gill et al.¹ and furthered by Ellison, Tuck, and Vaida.² The resulting aerosol was described as an inverse micelle with the polar head carboxylic groups of the fatty acid (lipid, RCO₂H) oriented into the water droplet and the acyl chains oriented out toward the atmosphere. The role that these fat-coated aerosols play in atmospheric chemistry very much depends on the oxidation of the hydrophobic shell. Aerosol growth through uptake of water and volatile organic compounds will only occur when oxidized species are present in the fat coat.² Field work by Tervahattu and co-workers demonstrated that fat coats do exist on some marine and continental aerosols.^{3–5} The proposal of the formation of fat-coated, seawater aerosols and the subsequent discovery of such aerosols has prompted a surge in research trying to understand the physical and chemical properties of fatty acid monolayers from an atmospheric perspective, as detailed in a recent review article by Donaldson and Vaida.⁶

Time-of-flight secondary ionization mass spectrometry measurements performed by Tervahattu et al. showed not only that palmitic acid (C₁₅H₃₁COOH) is the most prevalent fatty acid but also that oleic acid (C₁₇H₃₃COOH) is the most prevalent unsaturated fatty acid found in the fat coats of marine aerosols.^{3,4} Furthermore, these measurements showed no indication of oxidized species on the surface of the aerosols, despite atmospheric lifetimes long enough to react with common oxidants. The authors suggested that the oxidation products may either evaporate from the surface or partition into the aqueous subphase.^{3–5}

By designing experiments to understand oxidation and possible replacement of surfactants at the air/water interface, we tackle questions involved in the atmospheric processing of the fat-coated aerosols. Palmitic acid and oleic acid monolayers spread at the air/water interface were used as a model system to represent the fat-coated aerosol. Sum frequency generation (SFG) vibrational spectroscopy provides a tool to study monolayer systems at the air/water interface, as presented in pioneering work by Shen and co-workers⁷ and the Eisenthal group.⁸

Our broad-bandwidth, SFG (BBSFG) spectroscopy experiment simultaneously probes spectral regions up to 500 cm⁻¹ in width by overlapping a picosecond 800-nm pulse with a spectrally broad femtosecond infrared pulse in space and time on the sample surface.^{9,10} The generation of signal from the anti-stokes Raman scattering off an infrared excited surface requires that selection rules for both spectroscopies be met, which leads to a requirement for a lack of inversion in the probed species. The breaking of symmetry at the interface provides this lack of inversion. The signal intensity from this surface-specific technique depends not only on number density but also on the orientation of molecules present at the interface. This broad-bandwidth technique allows for a vibrational spectrum to be obtained from each laser pulse, limiting data acquisition time and providing better signal-to-noise ratios than most scanning SFG systems. The rapid acquisition of spectra from the monolayer at the air/water interface allows monitoring of dynamic processes. SFG spectroscopy has been used to study lipid monolayers at the air/water interface in model biological systems, as recently reviewed by Chen et al.¹¹ In this work, we present an SFG study of lipid monolayers at the air/water interface developed to understand atmospheric processes.

Experimental Method

The BBSFG experimental setup, described elsewhere,^{9,10} is detailed briefly here. A single titanium:sapphire laser (Spectra Physics Tsunami) seeds and a single neodymium:yttrium lithium fluoride laser (Spectra Physics Evolution) pumps two 1-kHz regenerative amplifiers (Spectra Physics Spitfire) designed to generate a 2-ps beam and a 85-fs beam. The femtosecond beam is used in an optical parametric amplifier with a difference frequency generation crystal (Spectra Physics OPA-800F) to produce tunable infrared light. In this study, the optical parametric amplifier was tuned so that the spectral bandwidth was 300 cm⁻¹. By use of turning and focusing optics, the infrared beam and the picosecond 800-nm beam are overlapped spatially at the sample surface. Adjusting a retro-reflector on a micrometer stage in the 800-nm beam line allows the beams to be overlapped temporally, as well. The input energy of the 800-nm beam was 250 μJ/pulse. The infrared input energy was 8

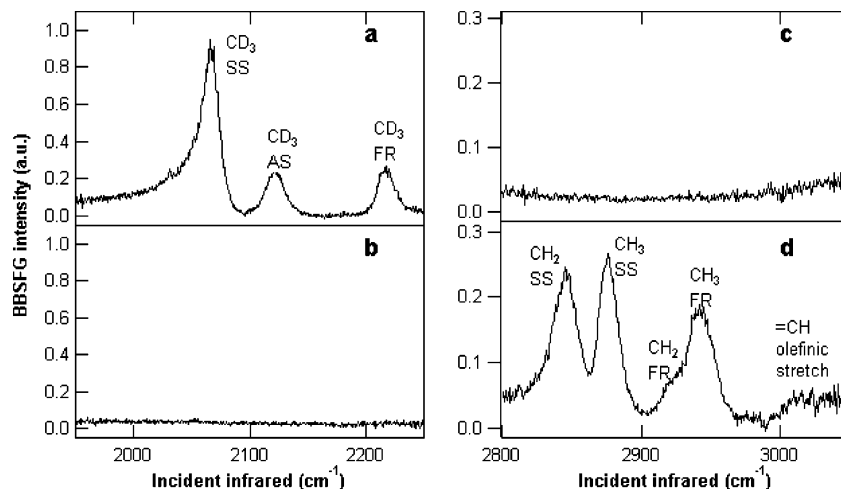


Figure 1. BBSFG spectra of d_{31} -palmitic acid and of protiated oleic acid monolayers. Panel (a) is the spectrum of the d_{31} -palmitic acid monolayer, showing the CD_3 symmetric stretching peak (2066 cm^{-1}), the CD_3 Fermi resonance (2121 cm^{-1}), and the CD_3 asymmetric stretch (2217 cm^{-1}). Panel (b) is the spectrum of the same monolayer represented in panel (a) 10 min after a monolayer equivalent of oleic acid is spread at the air/water interface. The absence of C–D stretching peaks indicates that the oleic acid has replaced the d_{31} -palmitic acid at the interface. Panel (c) is the spectrum of the d_{31} -palmitic acid monolayer taken in the C–H stretching region. In panel (d), the spectrum of protiated oleic acid spread at the air/water interface over the monolayer represented in panel (c) shows the CH_2 symmetric stretch (2846 cm^{-1}), the CH_3 symmetric stretch (2876 cm^{-1}), the CH_2 Fermi resonance (2923 cm^{-1}), the CH_3 Fermi resonance (2941 cm^{-1}), and the olefinic stretch from the CH stretching at the carbon–carbon double bond (3014 cm^{-1}). The rise in the baseline starting at approximately 3000 cm^{-1} is attributed to the SFG signal from the hydrogen-bonding network of water.

$\mu\text{J/pulse}$. The resulting SFG signal is detected in reflection at the output angle determined by the angle of the input beams and the conservation of angular momentum. The signal is spectrally dispersed using a monochromator (Acton Research SpectroPro 0.5 m) with the entrance and exit slits fully open and collected using a back-illuminated, liquid nitrogen cooled charge-coupled device (CCD, Roper Scientific 400 EB). Polarization optics for both the input beam lines and the signal detection line are used to select the polarization of these beams. All BBSFG data in this work were recorded in the SSP polarization combination for the SFG signal, the 800-nm beam, and the infrared beam, respectively. The spectra were background subtracted and normalized to the nonresonant SFG signal produced from a GaAs crystal.

Solutions of oleic acid and palmitic acid with a perdeuterated acyl chain (d_{31} -palmitic acid) were prepared in chloroform (99.8%, Sigma Aldrich, CAS 67-66-3). Oleic acid (99%, Sigma Aldrich, CAS 112-80-1) and d_{31} -palmitic acid (98%, Cambridge Isotopes, CAS 39756-30-4) were used as received without further purification. Monolayers were spread on 20 mL of deionized water with a resistivity of $18.3\text{ M}\Omega\text{-cm}$ (Barnstead Nanopure) in a Pyrex Petri dish. A $50\text{-}\mu\text{L}$ Hamilton syringe was used to spread the lipid solutions on the water surface. The quantity of fatty acid spread was equivalent to 20 \AA^2 per molecule, resulting in a monolayer in the condensed phase with well-organized acyl chains.¹² Ten minutes elapsed before BBSFG data acquisition began to allow the chloroform solvent to evaporate.

Ozone was generated by flowing O_2 (99.997%, Praxair) through a pen-ray lamp ozone generator (Jelight model 600). The concentration of ozone is calculated by measuring the absorbance at 254 nm (Ocean Optics USB 2000 spectrometer) and applying Beer's law, using the molar absorption coefficient of $1.15 \times 10^{-17}\text{ cm}^2/\text{molecule}$ ¹³ for the 10-cm path length. The O_2 flow was controlled using a mass flow controller (MKS Instruments 1479A51CS1BM). A second mass flow controller allows the introduction of N_2 (99.999%, Praxair) into the ozone stream to dilute the ozone concentration. The ozone concentra-

tion for all experiments in this work was approximately 20 ppm with a flow rate of 15 standard cubic centimeter per minute (sccm).

Results and Discussion

In this work, we take advantage of the differences in infrared vibrational energies between stretching modes of deuterated and protiated acyl chains of fatty acids. Tuning the optical parametric amplifier to the spectral region where CD_3 and CD_2 stretching modes are excited isolated spectral contributions from these molecules from their protiated counterparts. Figure 1a presents normalized BBSFG data taken with a 2-min acquisition time as a function of incident infrared wavelength of a d_{31} -palmitic acid monolayer spread at the air/water interface. The peaks in the spectrum can be attributed to the CD_3 symmetric stretch (2066 cm^{-1}), the CD_3 Fermi resonance (2121 cm^{-1}), and the CD_3 asymmetric stretch (2217 cm^{-1}), following assignments made by Yang et al.¹⁴ The absence of CD_2 symmetric and asymmetric stretching peaks indicates that the chains were well-aligned at the interface with no gauche defects.^{15,16} Following arguments made by Ma and Allen,¹⁶ we calculate the chain tilt to be roughly 20° from the surface normal. Figure 2a is a pictorial representation of the monolayer represented by the spectrum in Figure 1a.

To study replacement of the monolayer at the air/water interface, a 20 \AA^2 per molecule monolayer equivalent of protiated oleic acid was spread at the surface already bearing a d_{31} -palmitic acid monolayer. Initially, a lens forms on the surface, which disappeared after a couple of minutes. The longer carbon chain length and the presence of an unsaturated C=C bond make oleic acid less soluble in water than the slightly soluble palmitic acid, with solubilities of 1.15×10^{-5} and $8.21 \times 10^{-4}\text{ g/L}$, respectively.¹⁷ The protiated oleic acid replaced the d_{31} -palmitic acid monolayer on the surface. This is evidenced in Figure 1b, a 2-min spectrum where the C–D stretching peaks of the d_{31} -palmitic acid disappeared after spreading the protiated oleic acid on the d_{31} -palmitic acid monolayer represented in Figure 1a. With the optical parametric amplifier tuned to the

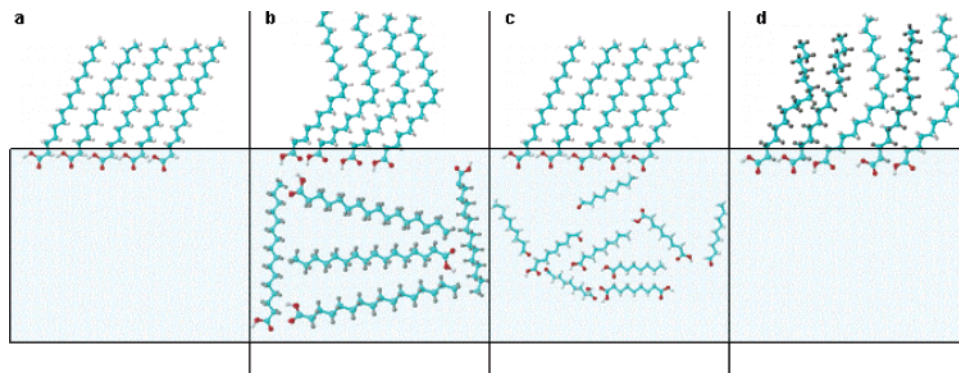


Figure 2. Schematic representation of monolayers at the air/water interface. Panel (a) is the representation of the d_{31} -palmitic acid monolayer. Panel (b) depicts the replacement of the d_{31} -palmitic acid monolayer with the oleic acid monolayer. Panel (c) illustrates the reformation of the d_{31} -palmitic acid monolayer after oxidation of oleic acid by ozone with the more polar and soluble oleic acid reaction products in the sub-phase. Panel (d) represents the mixed d_{31} -palmitic acid:oleic acid monolayer where the addition of oleic acid disrupts order of the palmitic acid chains.

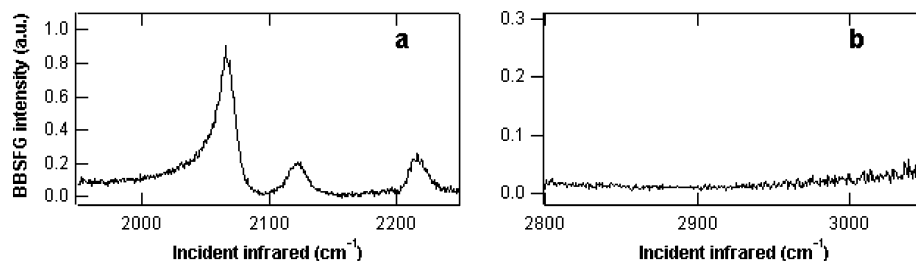


Figure 3. BBSFG spectra of d_{31} -palmitic acid and of oleic acid monolayers after oxidation of oleic acid with ozone. In panel (a), the monolayer of oleic acid at the air/water interface reacts with ozone, the initially displaced d_{31} -palmitic acid from the aqueous sub-phase re-forms a monolayer at the interface. In panel (b), the C–H stretching peaks of the protiated oleic acid monolayer are absent after oxidation with ozone.

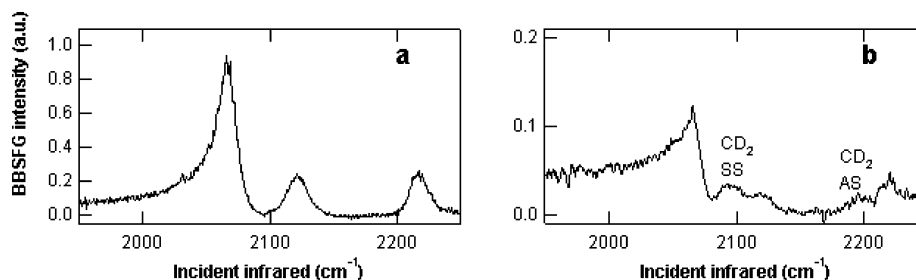


Figure 4. Sum frequency spectrum of mixed monolayer. Panel (a) is the pure d_{31} -palmitic acid monolayer shown in Figure 1a, replotted here for reference. In panel (b), the spectrum of a monolayer of 1:1 d_{31} -palmitic acid:oleic acid spread at the air/water interface shows both a decrease in signal intensity and an appearance of CD_2 stretching peaks, indicating that the presence of the oleic acid is disrupting the order of the palmitic acid chains.

C–D stretching region, the experiment is spectrally blind to the C–H stretching peaks from the oleic acid that occur between 2800 and 3050 cm^{-1} . Tuning the optical parametric amplifier to the C–H stretching region, however, confirmed that the oleic acid spectrum was present when the oleic acid replaced the palmitic acid monolayer, as demonstrated in parts c and d of Figure 1. Figure 1c is the spectrum of a d_{31} -palmitic acid monolayer taken in the C–H stretching region. Figure 1d is the spectrum of an oleic acid monolayer spread over the d_{31} -palmitic acid monolayer. The peaks present in the oleic acid spectrum in Figure 1d are the CH_2 symmetric stretch (2846 cm^{-1}), the CH_3 symmetric stretch (2876 cm^{-1}), the CH_2 Fermi resonance (2923 cm^{-1}), the CH_3 Fermi resonance (2941 cm^{-1}), and the olefinic =CH stretch at the carbon–carbon double bond (3014 cm^{-1}), following assignments and arguments made by Wang and co-workers¹⁸ and commonly known infrared and Raman vibrational assignments.¹⁹ The rise in the baseline starting at approximately 3000 cm^{-1} is attributed to the SFG signal from the hydrogen-bonding network of water.²⁰ These spectra prove that at equilibrium spreading pressure, less soluble surfactants replace more soluble surfactants at the air/water

interface. Figure 2b is a representation of the oleic acid monolayer replacing the d_{31} -palmitic acid at the surface and forcing the d_{31} -palmitic acid into the aqueous subphase.

To study oxidation of the unsaturated surfactants, ozone was introduced over the monolayer. While unsaturated hydrocarbons such as oleic acid react rapidly with this common tropospheric oxidant, saturated hydrocarbons such as palmitic acid do not react with ozone.¹³ Ozone at a concentration of 20 ppm flowed over the monolayer for 2 h. BBSFG spectra were taken with 30-s acquisition times to monitor the reaction. The C–D stretching peaks from the d_{31} -palmitic acid began to reappear in the BBSFG spectra after only 7 min. The extended oxidation time ensured that all of the oleic acid was oxidized. In the BBSFG spectra presented in Figure 3a, the peaks of d_{31} -palmitic acid are present after oxidation of the overlaid oleic acid monolayer, indicating that the products of the oleic acid oxidation are no longer present at the air/water interface, having been replaced by the d_{31} -palmitic acid from the subphase. Figure 3b is the spectrum after oxidation of the protiated oleic acid film taken in the C–H stretching region. These spectra are of the monolayers depicted in parts b and d of Figure 1 after

oxidation. The gas-phase reaction of oleic acid with ozone produces nonanal, nonanoic acid, azelaic acid, and 9-oxo-nonanoic acid.²¹ The solubilities of these species are 9.2×10^{-2} , 2.8×10^{-1} , 2.4, and 19 g/L, respectively.^{22,23} The solubility of palmitic acid is 8.21×10^{-4} g/L.¹⁷ The nonanal is volatile at room temperature and may evaporate into the gas phase. The soluble species can partition into the subphase, as demonstrated by Mmerekki et al. in work studying oxidation of anthracene at the air/water interface.²⁴ Once again, the results indicate that the least-soluble species is present on the surface.²⁵ The resurfacing of the d_{31} -palmitic acid monolayer after oxidation of the oleic acid monolayer is depicted in Figure 2c, with the soluble reaction products now in the aqueous subphase.

To further prove the conclusion that the oleic acid was completely oxidized and replaced by the d_{31} -palmitic acid, the spectrum of a 1:1 d_{31} -palmitic acid:oleic acid solution spread at the air/water interface is presented in Figure 4b. Figure 4a is the spectrum shown in Figure 1a, replotted here for reference. The intensity of the SFG signal is much lower for the mixed monolayer than the pure d_{31} -palmitic acid monolayer, a result of both the lower number of d_{31} -palmitic acid molecules in the monolayer and the change in orientation of these molecules. In Figure 4b, not only is the signal level lower but also the CD_2 stretching (2096 cm^{-1}) and asymmetric peaks (2197 cm^{-1})¹⁴ are clearly visible, indicating that the d_{31} -palmitic acid in the monolayer was no longer well-ordered and aligned.^{15,16} The presence of the oleic acid in the film is causing the disruption of order. Figure 2d depicts a representation of the disorder present in the mixed monolayer. The absence of the CD_2 stretching peaks coupled with the return in signal intensity of the CD_3 stretching peaks in the d_{31} -palmitic acid monolayer spectrum in Figure 3a confirms the conclusion that oleic acid was no longer present at the air/water interface and that a well-ordered d_{31} -palmitic acid monolayer was present.

Conclusions

The studies presented in this work support the conclusions of Tervahattu and co-workers³⁻⁵ that fatty acid coats on marine aerosols could react with tropospheric oxidants and, yet, have no oxidized species on the surface. If the products of oxidation are more soluble than species residing in the subphase, then the least soluble species would replace the oxidation products on the surface. Oxidation produces hydrocarbons with oxygen-containing functional groups, which are more soluble in water than their parent species. Similar results are expected with the oxidation of hydrocarbons by hydroxyl radical, another major tropospheric oxidant. For example, hydroxyl radical reactions with hexadecane produced hexadecanone, short-chain aldehydes, and short-chain carboxylic acids.²⁶ These oxidation products are all more soluble in water than the unoxidized starting reagent. Unoxidized species from the subphase should continue to replace oxidation products at the surface until all unoxidized species

are depleted. Only then will there be oxidized species at the air/water interface of the aerosol. It is also plausible that once the monolayer on the aerosol is partially oxidized, the aqueous core will no longer be protected from the atmosphere and may evaporate or fragment.

Acknowledgment. L. F. V. acknowledges support through a Camille and Henry Dreyfus Environmental Chemistry Postdoctoral Fellowship. We also acknowledge the National Science Foundation (ATM-0413893 and CHE-0089147) for funding this work. We also thank J. Beck for assistance in producing the graphic image submitted as cover art.

References and Notes

- (1) Gill, P. S.; Graedel, T. E.; Weschler, C. J. *Rev. Geophys. Space Phys.* **1983**, *21*, 903.
- (2) Ellison, G. B.; Tuck, A. F.; Vaida, V. *J. Geophys. Res.* **1999**, *104*, 11633.
- (3) Tervahattu, H.; Juhanaja, J.; Kupiainen, K. *J. Geophys. Res.* **2002**, *D16*, ACH18/1.
- (4) Tervahattu, H.; Hartonen, K.; Kerminen, V.-M.; Kupiainen, K.; Aarnio, P.; Koskentalo, T.; Tuck, A. F.; Vaida, V. *J. Geophys. Res.* **2002**, *D7 & D8*, AAC 1/1.
- (5) Tervahattu, H.; Juhanaja, J.; Vaida, V.; Tuck, A. F.; Niemi, J. V.; Kupiainen, K.; Kulmala, M.; Vehkamaki, H. *J. Geophys. Res.* **2005**, *110*, D06207/1.
- (6) Donaldson, D. J.; Vaida, V. *Chem. Rev.* **2006**, *106*, 1445.
- (7) Guyot-Sionnest, P.; Hunt, J. H.; Shen, Y. R. *Phys. Rev. Lett.* **1987**, *59*, 1597.
- (8) Vogel, V.; Mullin, C. S.; Shen, Y. R.; Kim, M. W. *J. Chem. Phys.* **1991**, *95*, 4620.
- (9) Hommel, E. L.; Ma, G.; Allen, H. C. *Anal. Lett.* **2001**, *17*, 1325.
- (10) Ma, G.; Allen, H. C. *J. Phys. Chem. B* **2003**, *107*, 6343.
- (11) Chen, X.; Clarke, M. L.; Wang, J.; Chen, Z. *Int. J. Mod. Phys. B* **2005**, *19*, 691.
- (12) Albrecht, O.; Matsuda, H.; Eguchi, K.; Nakagiri, T. *Thin Solid Films* **1999**, *338*, 252.
- (13) Finlayson-Pitts, B. J.; Pitts, J. N., Jr. *Chemistry of the Upper and Lower Atmosphere*; Academic Press: New York, 2000.
- (14) Yang, C. S. C.; Richter, L. J.; Stephenson, J. C.; Briggman, K. A. *Langmuir* **2002**, *18*, 7549.
- (15) Holman, J.; Neivandt, D. J.; Davies, P. B. *Chem. Phys. Lett.* **2004**, *386*, 60.
- (16) Ma, G.; Allen, H. C. *Langmuir* **2006**, *22*, 5341.
- (17) Howard, P. H.; Meylan, W. M. *Handbook of Physical Properties of Organic Chemicals*; Lewis Publishers: New York, 1997.
- (18) Lu, R.; Gan, W.; Wu, B.-H.; Zhang, Z.; Guo, Y.; Wang, H.-F. *J. Phys. Chem. B* **2005**, *109*, 14118.
- (19) Socrates, G. *Infrared and Raman Characteristic Group Frequencies*, 3rd ed.; John Wiley and Sons: Limited: New York, 2001.
- (20) Liu, D.; Ma, G.; Levering, L. M.; Allen, H. C. *J. Phys. Chem. B* **2004**, *108*, 2252.
- (21) Moise, T.; Rudich, Y. *J. Phys. Chem. A* **2002**, *106*, 6469.
- (22) Yalkowsky, S. H.; He, Y. *Handbook of Aqueous Solubility Data*; CRC Press: Washington D. C., 2003.
- (23) King, G. *J. Chem. Soc.* **1938**, 1826.
- (24) Mmerekki, B. T.; Donaldson, D. J.; Gilman, J. B.; Eliason, T. L.; Vaida, V. *Atmos. Environ.* **2004**, *38*, 6091.
- (25) Wadia, Y.; Tobias, D. J.; Stafford, R.; Finlayson-Pitts, B. J. *Langmuir* **2000**, *16*, 9321.
- (26) Eliason, T. L.; Gilman, J. B.; Vaida, V. *Atmos. Environ.* **2004**, *38*, 1367.